CHAPTER IV
RESULTS AND DISCUSSION

4.1 Characterization of Vegetable oil

The refined palm oil was used in this work. Table 4.1 shows the properties of refined palm oil such as density, kinematic viscosity, free fatty acid content, moisture content and fatty acid composition. According to Thai Industrial Standard (TIS 203-2520), an edible virgin oil has been defined as an oil obtained by mechanical or thermal processes and may have been purified by washing, setting, filtering or centrifuging. The refined oil are allowed to have acid value not exceeding 4 mg KOH/g and the moisture content is not exceed 0.2%. And industrial vegetable oil is oil which is not edible with acid value of 10 mg KOH/g of oil and moisture content is not higher than 0.5%.

Table 4.1 Properties of palm oil

Properties	Palm oil
Density at 27°C (g/ml)	0.901
Kinematic Viscosity (cSt)	40.5155
Free fatty acid (%)	0.3579
Moisture Content (ppm)	452.8

The free fatty acid composition of palm oil analyzed by a gas chromatograph is shown in Figure 4.1 and the composition of fatty acid in the palm oil is given in Table 4.2. The major fatty acid components for palm oil are oleic acid and palmitic acid. Based on these compositions, the molecular weight of palm oil of about 850 g/mole was calculated and obtained.

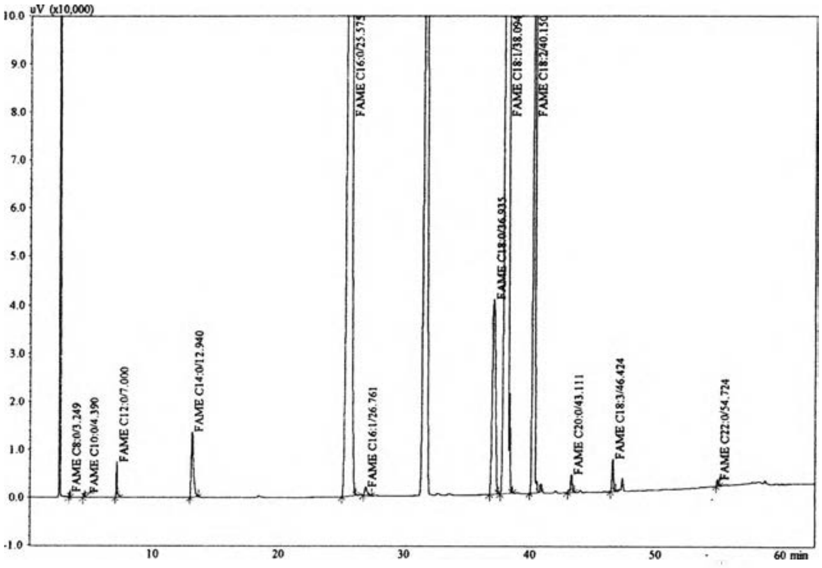

Figure 4.1 Chromatogram of palm oil.

Table 4.2 Fatty acid composition of palm oil

Fatty acid	Wt%
Caprylic acid (C8:0)	0.01
Capric acid (C10:0)	0.01
Lauric acid (C12:0)	0.20
Myristic acid (C14:0)	0.83
Palmitic acid (16:0)	40.29
Stearic acid (C18:0)	3.70
Oleic acid (C18:1)	43.73
Linoleic acid (C18:2)	10.64
Linolenic acid (C18:3)	0.19
Arachidic acid (C20:0)	0.30

4.2 Catalyst Characterization

4.2.1 X-ray Diffraction (XRD)

4.2.1.1 XRD Patterns of Spent KOH/ZrO₂ Catalysts

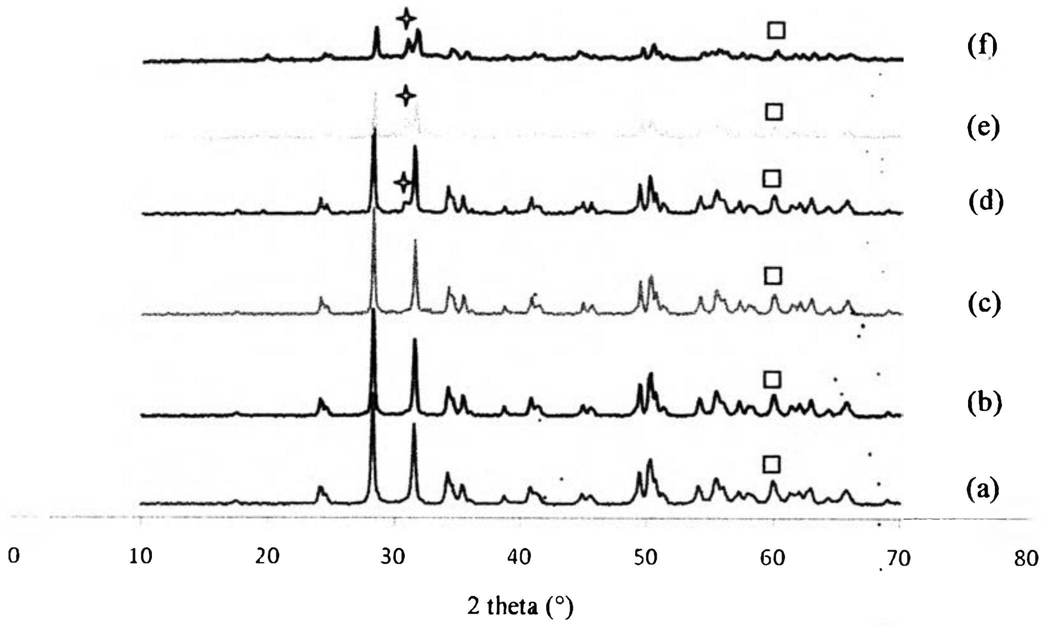

Figure 4.2 XRD patterns of ZrO_2 and KOH/ZrO_2 catalysts: (a) ZrO_2; (b) 10 wt.% K/ZrO_2, (c) 15 wt.% K/ZrO_2, (d) 20 wt.% K/ZrO_2, (e) 25 wt.% K/ZrO_2, (f) 30 wt.% K/ZrO_2, ✧K_2O, □cubic.

The XRD patterns of ZrO_2 and KOH/ZrO_2 with various loading of K are shown in Figure 4.2. The XRD pattern of fresh ZrO_2 shows the typical diffraction peaks at $2\theta = 28°$, 31°, 34°, 49°, 50°, 54°, 55° and 60°. It indicated the monoclinic phase of ZrO_2; however, cubic phase of ZrO_2 can be observed at $2\theta = 60.337°$ as cubic (311) plane of ZrO_2. When the loading amount of K was increased to 10 wt.% and 15 wt.%, the XRD patterns were almost the same as the XRD pattern of ZrO_2. And when the loading amount of K was further increased to 20 wt.%, the characteristic peak of K_2O were observed at $2\theta = 31°$, 39°, 51°, 55°, and 62° (Xie *et al.*, 2006). A new phase can be observed in 20 and 30 wt.% K/ZrO_2. This result agrees with the results of KOH/Al_2O_3 by Noiroj and KNO_3/Al_2O_3 (Xie *et al.*, 2006). Their showed that at low loading amount of K (10 wt.% and 15 wt.%), no K_2O peak was observed. In the present work indicated that the new phase of K_2O was observed; therefore, KOH can be well dispersed on the ZrO_2 support in the form of a monolayer at a low loading of K. It was also found that the XRD results show mostly monoclinic phase retained in the nanostructured ZrO_2 of KOH/ZrO_2 samples and was a part of catalytic active site to convert the triglyceride to mono alkyl ester. When the loading amount of K was increased, the intensity of K_2O peak further increased. It could be concluded that the catalyst might have more active sites. As a consequence, the catalyst has more activity. These results agree well with the result of KNO_3/Al_2O_3 reported by Xie *et al.* (2006). They explained that at low KNO_3 loading, the XRD patterns are identical to that of Al_2O_3 because of the good dispersion of KNO_3 on Al_2O_3. From the XRD results, when the KOH loading was increased to 20-25 wt.%, the new phase of K_2O was observed. From Figure 4.2, when loading amount of K was raised to 25 wt.% K/ZrO_2, the XRD peak of KOH appeared on the XRD patterns at $2\theta = 30.48°, 33.28°, 45.79°$. The presence of KOH peak implied that a residual phase of KOH remained on the sample and the KOH spontaneously dispersed on ZrO_2. Moreover, when loaded KOH more than the spontaneous dispersion capacity, KOH was difficult to decompose to the active sites. The undetected peak of KOH at low loading amount of K can be suggested that phase of KOH dispersed as a monolayer on the surface of ZrO_2 (Xie *et al.*, 2006). In addition, the intensity of KOH/ZrO_2 peak decreased with increasing the loading amount of K.

4.2.1.2 XRD Patterns of Spent KOH/mordenite Catalysts

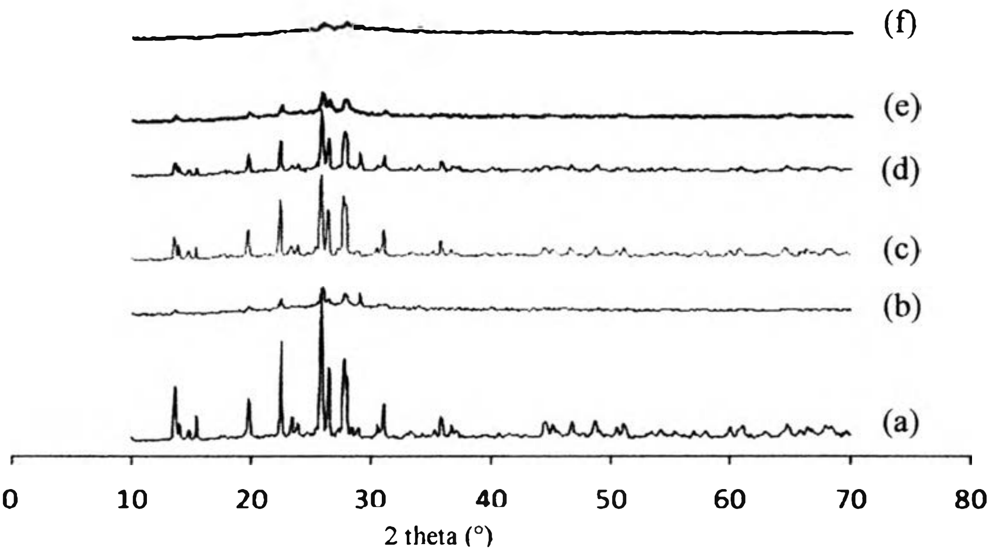

Figure 4.3 XRD patterns of mordenite and K/mordenite catalysts: (a) mordenite, (b) 5 wt.% K/mordenite, (c) 10 wt.% K/mordenite, (d) 15 wt.% K/mordenite, (e) 20 wt.% K/mordenite, (f) 30 wt.% K/mordenite.

The X-ray diffraction analysis of KOH/mordenite was investigated and the structure are illustrated in Figure 4.3. The result shows that when the loading amount of K was increased from 10 wt.% to 20 wt.% , the XRD pattern showed the same XRD pattern as the mordenite. The XRD pattern of fresh mordenite shows the diffraction peak at 2θ = 9.7, 13.5, 19.6, 22.3, 25.7, 26.3, 27.5, and 30.9°. The XRD patterns of 10 wt.%, 15 wt.%, and 20 wt.% K show that the intensity of mordenite peak decreased when increasing the loading amount of K. The similarity XRD patterns of different loads of K on mordenite and mordenite support gave the advantage on the crystalline structure due to it remained the pore site which KOH can diffuse into it. This result was supported by the experiment of Xie and Li (2006). They suggested that using KOH could keep the pore structure of zeolites that would be necessary for catalysis. Moreover, the K_2O was not observed on the XRD pattern of KOH/mordenite. It can be sugested that the intensity of K_2O peak was very low as compare to the XRD patterns of mordenite zeolite due to the mordenite has high crystalline sturcture. In addition, the presence of K_2O could not be confirmed in this XRD pattern due to the significant overlab of its reflechtions with theses of the mordenite. At high loading amounts of K (30 wt.%), the XRD pattern of the catalyst showed an increased in amorphus part. This effect could be caused by KOH destroyed the structure of zeolite.

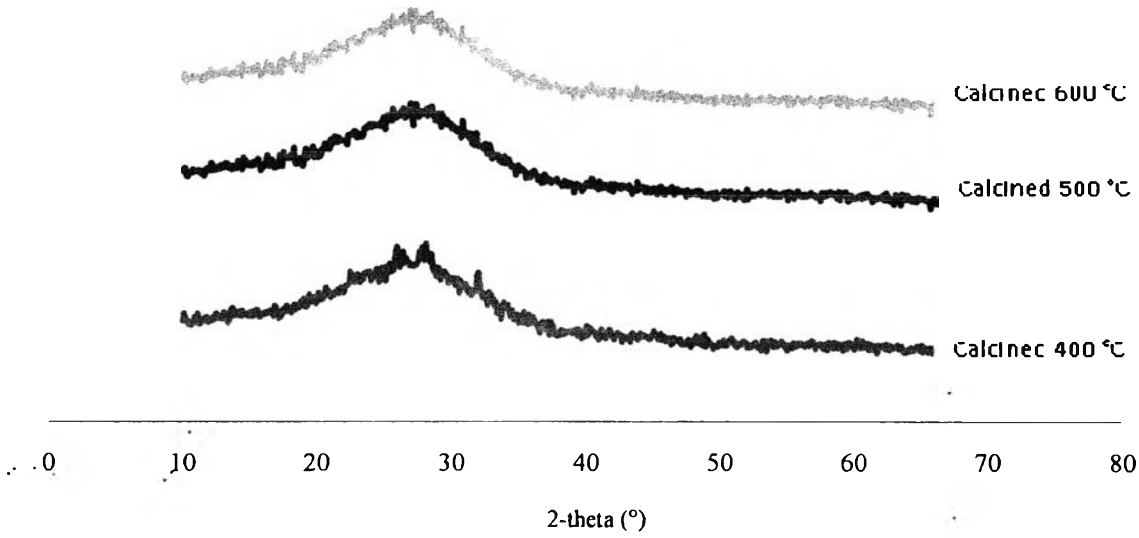

Figure 4.4 XRD patterns of 20 wt.% K/mordenite catalysts with various calcination temperatures.

Figure 4.4 shows the XRD pattern of KOH/mordenite with various calcination temperature. The XRD pattern of the calcined samples at 400, 500, and 600°C coresponds with the same as the XRD pattern of the uncalcined sample. However, the calcination peocedure of mordenite at a temperature of 500°C, yield and amorphous phase. It can be suggest that at high calcination temperature the structure of mordenite was collapsed (Zhu *et.al.*, 1995)

4.2.2 Scanning Electron Microscopy with Energy Dispersive Spectrometer

4.2.2.1 KOH/ZrO₂ Catalysts

The morphology of ZrO_2 support and fresh KOH/ZrO_2 catalysts are presented in Figure 4.5.

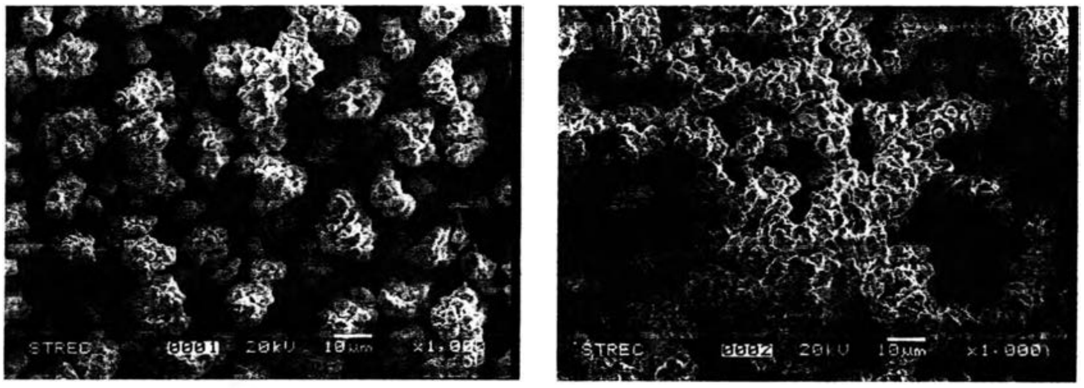

(a) Fresh ZrO_2 (b) Fresh 5 wt.% K/ZrO_2

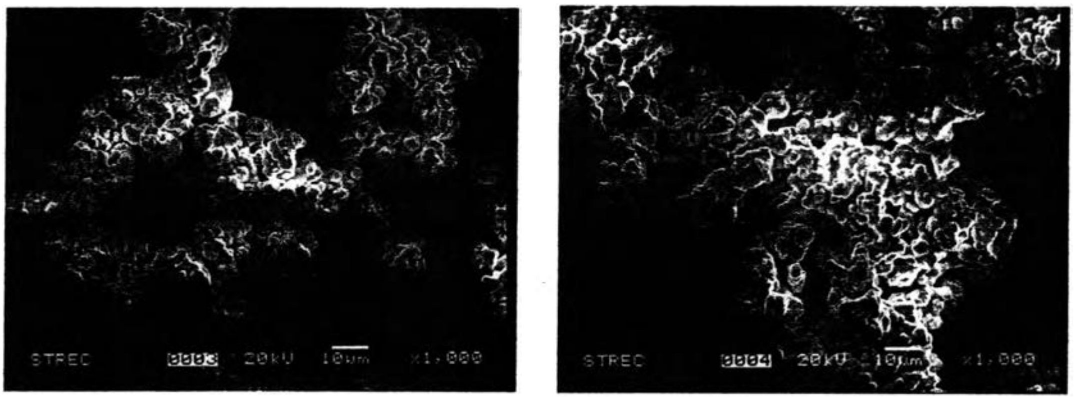

(c) Fresh 10 wt.% K/ZrO_2 (d) Fresh 15 wt.% K/ZrO_2

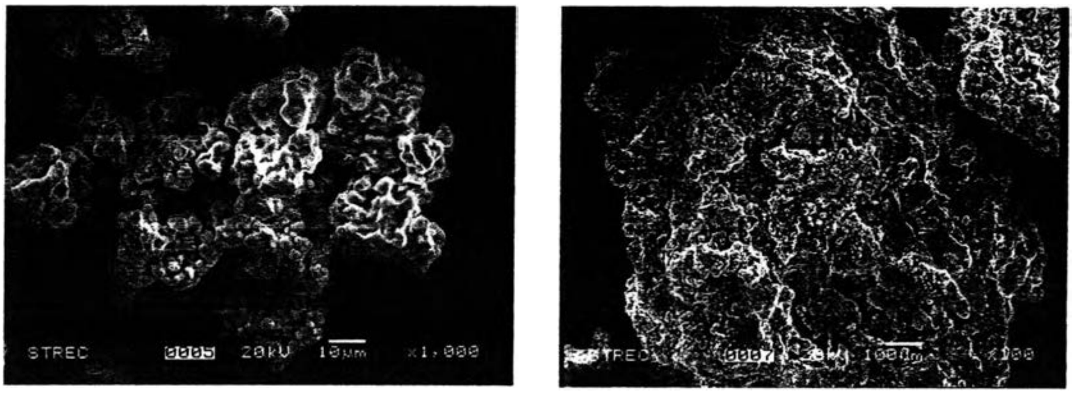

(e) Fresh 20 wt.% K/ZrO_2 (f) Fresh 25 wt % K/ZrO_2

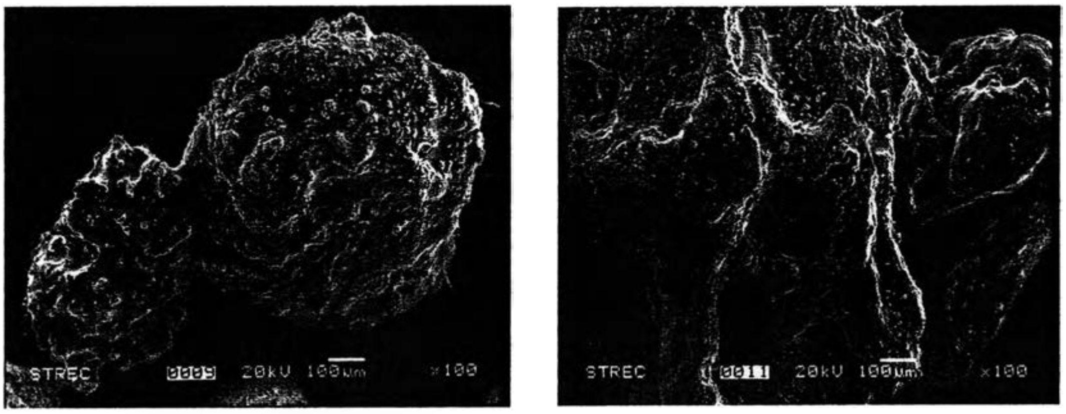

(f) Fresh 30 wt.% K/ZrO_2 (g) Fresh 35 wt.% K/ZrO_2

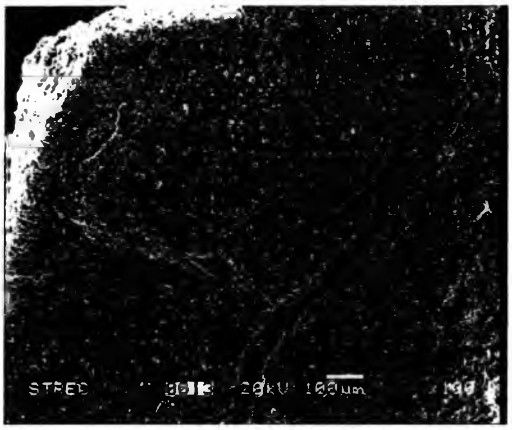

(h) Fresh 40 wt.% K/ZrO_2

Figure 4.5 SEM images of ZrO_2 support and fresh KOH/ZrO_2 with various K loadings.

Scanning electron microscopy has extensively been used for examination of the topology of catalyst surfaces. Figure 4.5 shows the SEM pictures (with scale bar ~10µm) that the particles of fresh ZrO_2 are clumpy agglomerated and spherical in shape with an average size in the range 5-15 µm. The KOH/ZrO_2 showed the agglomeration of small particles as the K loading; however, the morphology of the KOH/ZrO_2 is similar to the ZrO_2 sample. When the loading amount of K was increased from 5 wt.% to 20 wt.%, the particles sizes were increased from 10 µm to 100 µm. Thus this can be suggested that a good dispersion of KOH on ZrO_2 retained its structure which is important for the catalysis and therefore the potassium species was found highly distributed upon the surface of the support. And when wt.% loading of K was increased to 30-40 wt.%, the size of crystallize was increased because KOH covered the particle of ZrO_2 support. As evidenced by Figure 4.5, the structure of 30 to 40 wt.% K loaded on ZrO_2 was destroyed by high concentration of KOH because of the recrytallization of porous ZrO_2 (Xei *et al.*, 2007). Therefore, when wt.% loading amount of KOH was increased, the surface area of fresh KOH/ZrO_2 catalyst was decreased because the crystallites size was larger. The SEM results are in good correspondence with the XRD results obtained on the different samples.

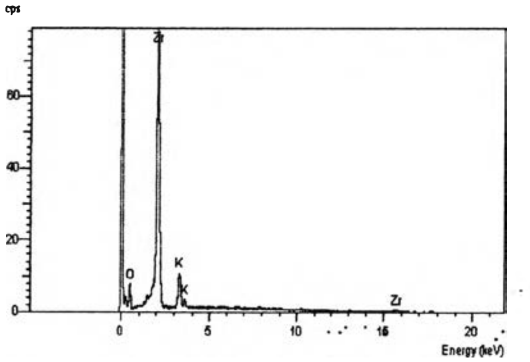

(c) Fresh 10 wt.% K/ZrO_2

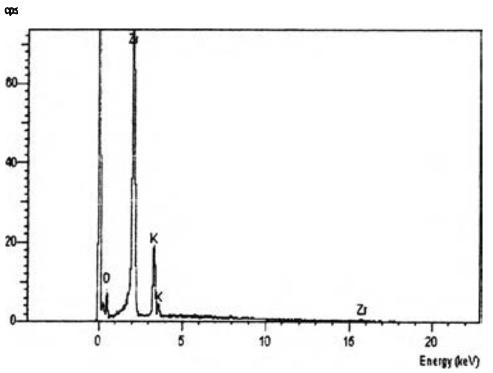

(d) Fresh 15 wt.% K/ZrO_2

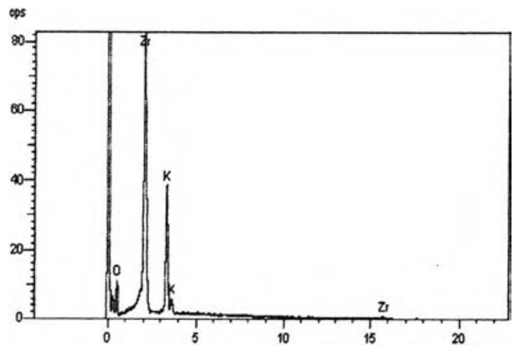

(e) Fresh 20 wt.% K/ZrO_2

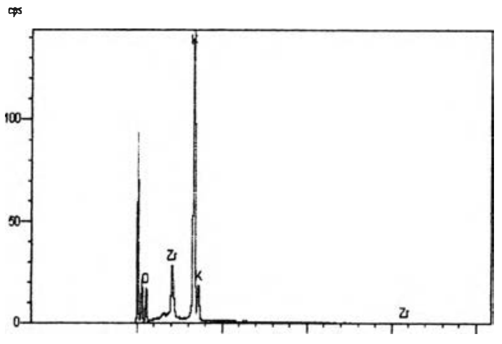

(f) Fresh 25 wt.% K/ZrO_2

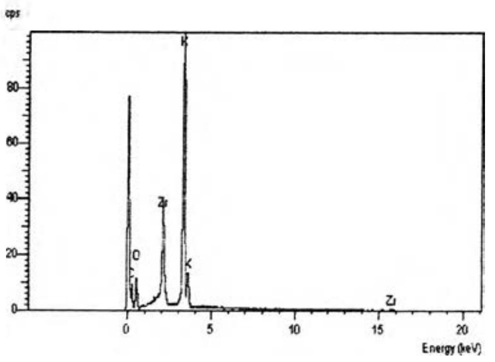

(g) Fresh 30 wt.% K/ZrO_2

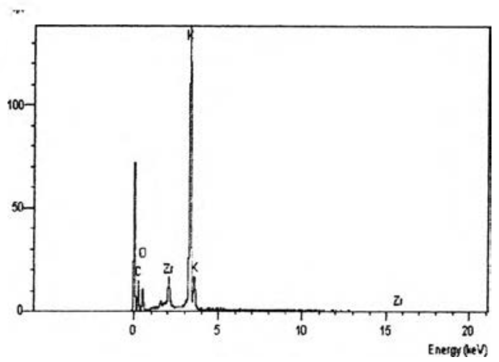

(h) Fresh 35 wt.% K/ZrO_2

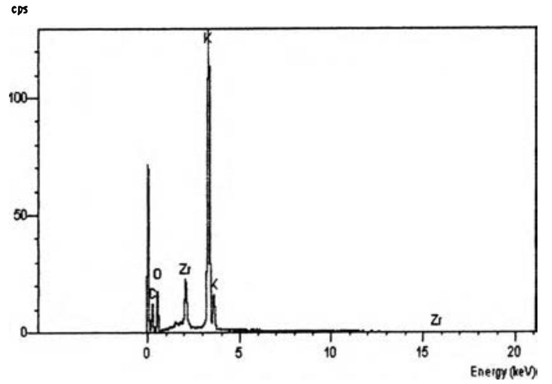

(i) Fresh 40 wt.% K/ZrO_2

Figure 4.6 EDS results of fresh ZrO_2 and KOH/ZrO_2 with various K loadings.

The chemical composition of ZrO_2 might be changed since the KOH was used to impregnate on its structure. Which EDS was used to analyze the chemical compound of ZrO_2 support. The spectrograms of them are shown in Figure 4.6. The graph indicated that the peak of O and Zr appeared at 0.5 and 1 keV, respectively. After KOH was loaded on the ZrO_2 support, the peak of potassium (K) element appeared at 3.2 and 3.5 keV. Furthermore, when the wt.% K loading was further increased, the intensity of K was increased. The maximum intensity at 155 cps was obtained with 35 wt.% K/ZrO_2. This result is in good correspondence with the SEM result. When the intensity of potassium (K) element increased, the potassium might be covered the ZrO_2 support which made the particle larger with consequent decreased the surface area to volume.

4.2.2.2 KOH/mordenite Zeolite Catalysts

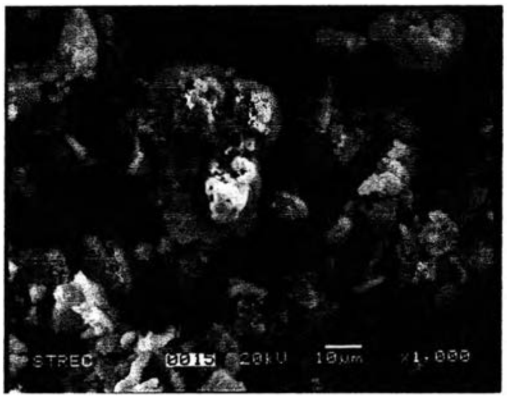

(a) Uncalcined mordenite

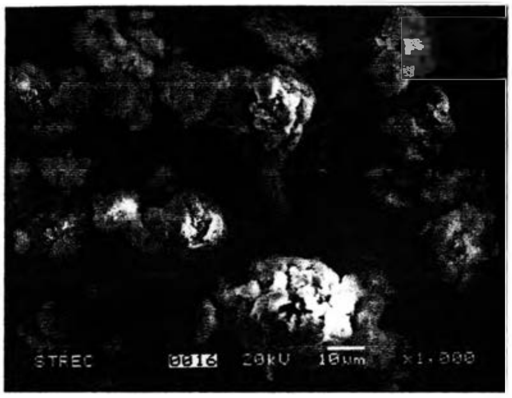

(b) Fresh 5 wt.% K/mordenite

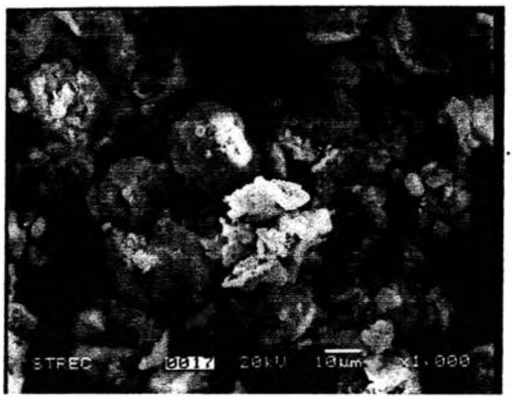

(c) Fresh 10 wt.% K/mordenite

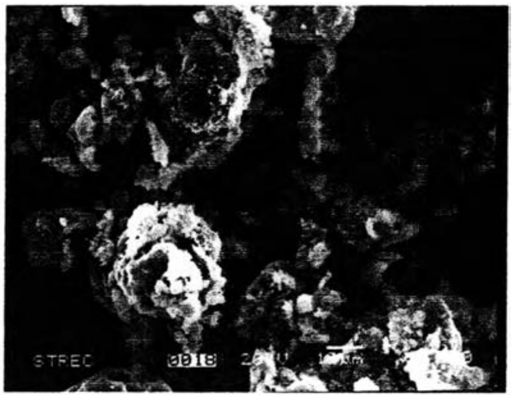

(d) Fresh 15 wt.% K/mordenite

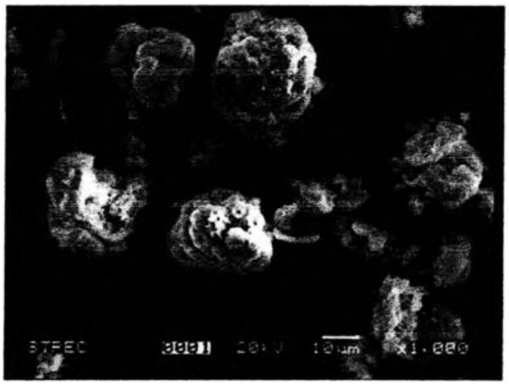

(e) Fresh 20 wt.% K/mordenite

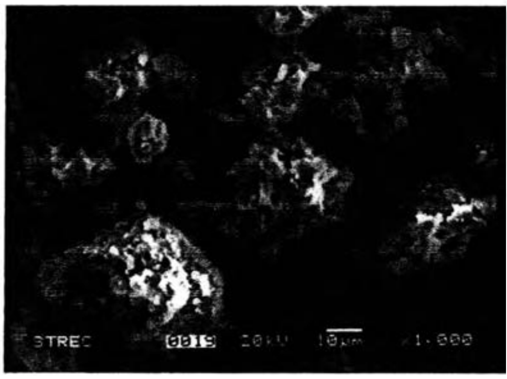

(f) Fresh 25 wt.% K/mordenite

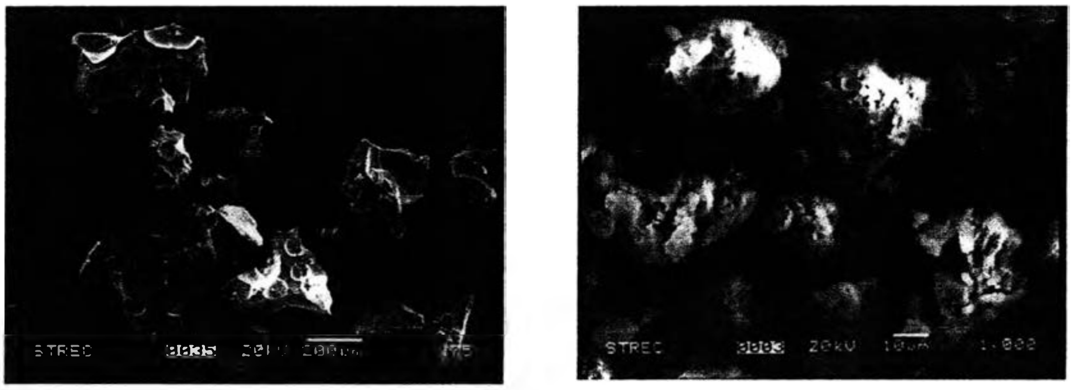

(g) Fresh 30 wt.% K/mordenite (h) 20 wt.% calcined 400°C

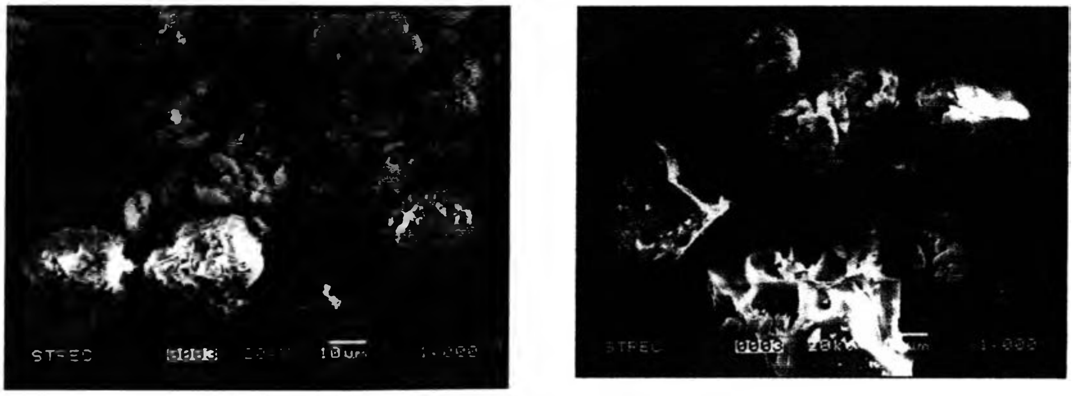

(i) 20 wt.% calcined 500°C (j) 20 wt.% calcined 600°C

Figure 4.7 SEM images of mordenite and fresh KOH/mordenite catalysts with various K loadings, and various calcination temperatures.

The SEM images revealed that the mordenite and KOH/mordenite particles were almost spherical in shape with dimension about 10-20 μm, as shown in Figure 4.7. No significant difference in morphology of mordenite and KOH/mordenite were observed. After being loaded with K, the KOH/mordenite catalyst retained its structures. But the particle size of the catalyst increased with increasing the loading amount of K. It means that the surface area of the catalyst decreased. However, at high loading amount of K on mordenite (30 wt.%), the morphology was changed to amorphous due to the destroyed structure of mordenite support. After being impregnated with K, the prepared catalysts were calcined with different temperatures by varying temperature in the range 400 to 600°C. The SEM results shown in Figure 4.6 (h-j), the catalysts calcined at 400 and 500°C showed no significant difference from uncalcined catalyst. However, the morphology of catalyst calcined at 600°C showed a slightly change with decreasing crystallinity.

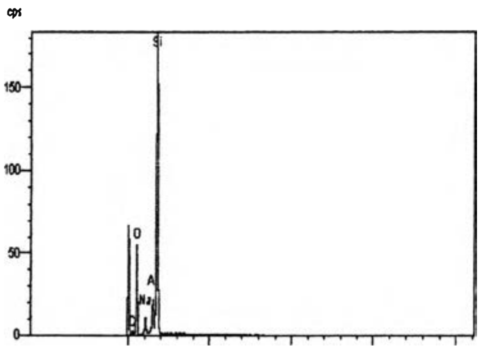

(a) mordenite

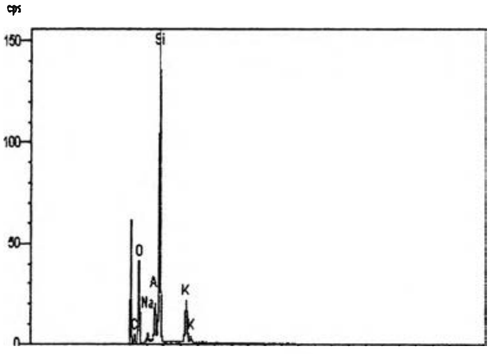

(b) Fresh 5 wt.% K/mordenite

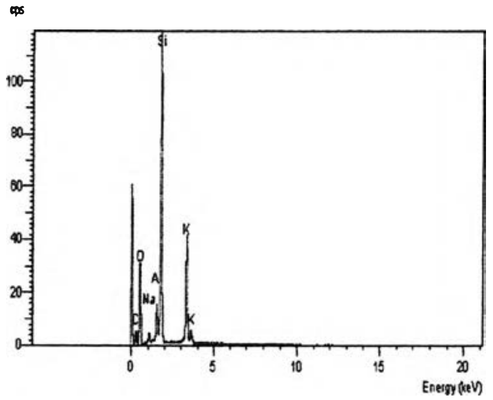

(c) Fresh 10 wt.% K/mordenite

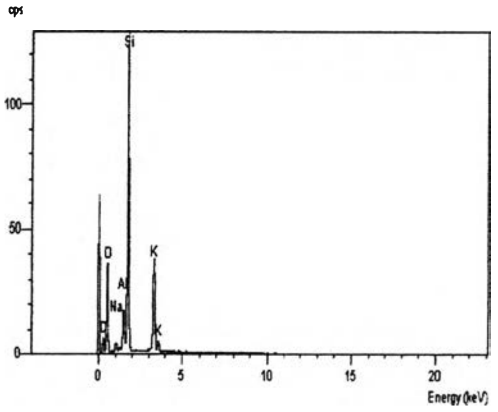

(d) Fresh 15 wt.% K/mordenite

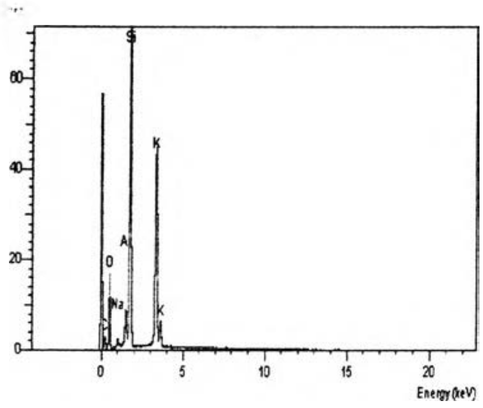

(e) Fresh 20 wt.% K/mordenite

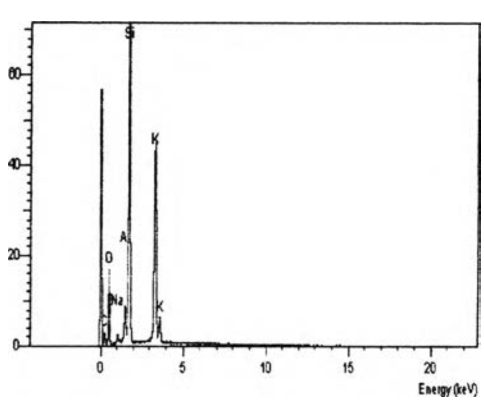

(f) Fresh 25 wt.% K/mordenite

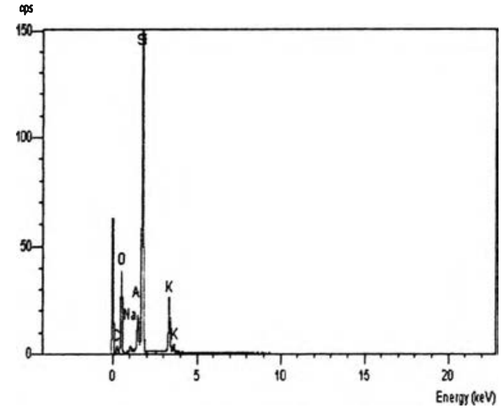

(g) Spent 15 wt.% K/mordenite

Figure 4.8 EDS of mordenite and fresh KOH/mordenite catalysts with various K loadings.

The chemical composition of mordenite zeolite was detected by EDS. The different structure of unmodified mordenite zeolite support and modified mordenite zeolite are shown in Figure 4.8. The spectrogram of the unmodified mordenite zeolite support indicated that the content of O, Na, Al and Si appeared at 0.5, 1, 1.7 and 1.9 keV, respectively. After being impregnated with KOH on mordenite zeolite, the peak of potassium (K) element appeared at 3.2 and 3.5 keV. When wt.% K loading was decreased, the intensity of potassium (K) element was higher. The highest intensity of potassium element were observed with 25 wt.% KOH/mordenite. The results of EDS related to the results of SEM which the higher wt.% K loading, the higher intensity of potassium (K) element and the bigger particle size which affected to the smaller surface area to volume because KOH might cover on mordenite support.

4.3 Transesterification Reaction

The KOH/ZrO_2 and KOH/mordenite catalysts were used as a heterogeneous catalyst in transesterification reaction. To study the optimum condition of these catalysts in transesterification of refined palm oil, the staring condition of transesterification reaction in KOH/ZrO_2 and KOH/mordenite catalysts were reaction temperature of 65°C, 20 wt.% loading amount of K on ZrO_2 and mordenite support with a molar ratio of methanol to oil of 15:1, 3 wt.% of the catalyst (base on weight of the vegetable oil), a stirrer speed of 300 rpm.

4.3.1 Influence of Catalyst Size on the Methyl Ester Content

To study the influence of the particle size of catalyst on the methyl ester content, various size of KOH/ZrO_2 catalysts were tested. The initial condition was carried out at reaction temperature of 65°C, reaction time 1 hour, 20 wt.% loading amount of K on ZrO_2 support at a molar ratio of methanol to oil of 15:1, 3 wt.% of the catalyst (base on weight of the vegetable oil) and, a stirrer speed of 300 rpm. The methyl ester content at each size of catalyst is shown in Figure 4.9. The methyl ester content does not change drastically with size of catalyst; however, the methyl ester content increased with increasing particle size of catalyst. The maximum methyl ester content of 89.81 wt.% was obtained with 10-20 mesh. It is possible that the particle size may affect the pore size inside the catalyst. The KOH/ZrO_2 having the large pore size would exhibit a higher activity than a catalyst with the smaller pore size.

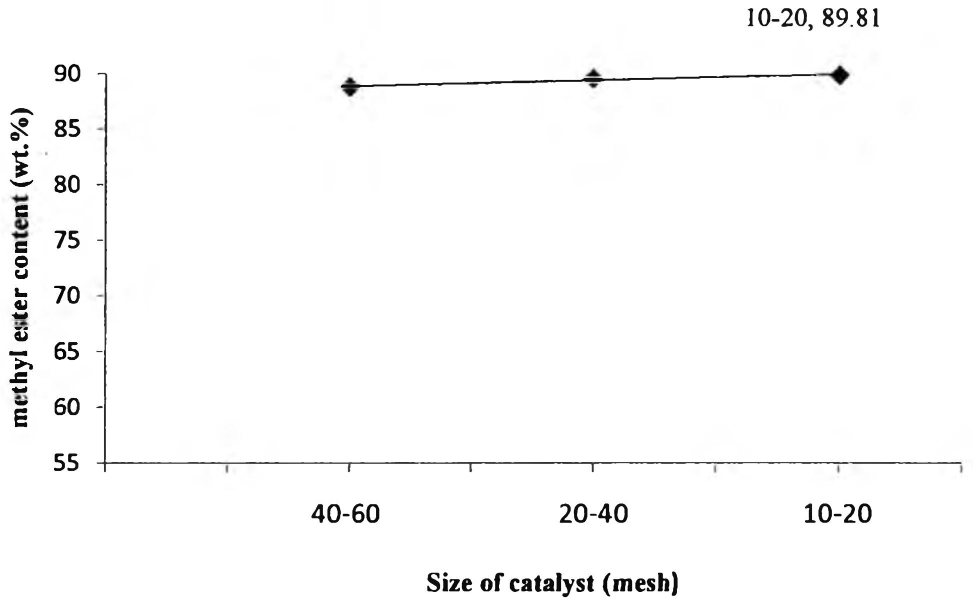

Figure 4.9 Influence of the catalyst size on the methyl ester content. Reaction condition: temperature of 65°C at 1 hours of reaction time, a molar ratio of methanol to oil of 15:1, 3 wt.% of the catalyst (base on weight of the vegetable oil), and a stirrer speed of 300 rpm.

4.3.2 Influence of Reaction Time on the Methyl Ester Content and Biodiesel Yield

The initial condition was carried out at 65°C of reaction temperature, the size of KOH/ZrO_2 catalysts was 10-20 mesh, 20 wt.% K on ZrO_2, a 15:1 molar ratio of methanol to oil, 3 wt.% of the catalyst, and 300 rpm of stirrer speed. The reaction time was varied within a range from 30 minutes to 5 hours. The dependence of the wt.% methyl ester content and wt.% yield on the reaction time can be seen from Figure 4.10. The percent yield of biodiesel yield increased at initial 30 minutes and afterward it remained constant until 5 hours, as a result of near equilibrium conversion. The results of methyl ester content showed that the methyl ester content slightly increased from 1 to 4 hours and slightly dropped at 5 hours. The highest methyl ester content and biodiesel yield obtained at 4 hours were 96.65 wt.% and 91.51 wt.%, respectively.

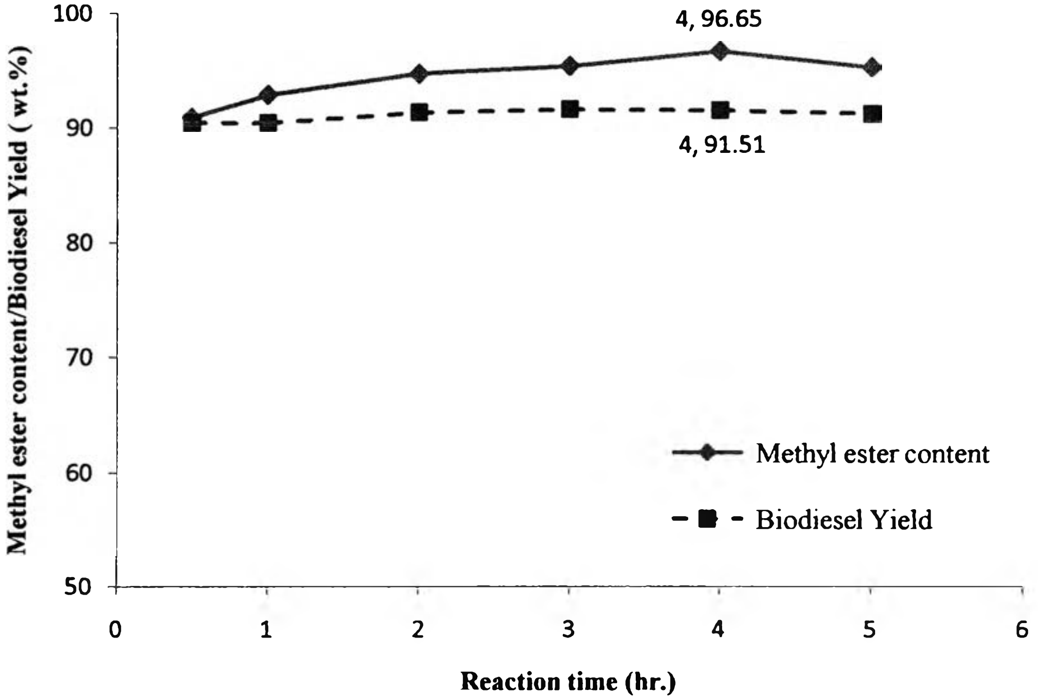

Figure 4.10 Influence of reaction time on the methyl ester content and biodiesel yield. Reaction condition: reaction temperature of 65°C, 20 wt.% loading amount of K on ZrO_2 support with a molar ratio of methanol to oil of 15:1, 3 wt.% of the catalyst (base on weight of the vegetable oil), a stirrer speed of 300 rpm, and the size of KOH/ZrO_2 catalysts was 10-20 mesh.

Influence of reaction time on the methyl ester content and biodiesel yield of KOH/mordenite catalyst was studied at reaction temperature of 65°C, 20 wt.% loading amount of K on mordenite with a molar ratio of methanol to oil of 15:1, 3 wt.% of the catalyst (base on weight of the vegetable oil), and a stirrer speed of 300 rpm. The reaction time was varied from 3 to 7 hours. As shown in Figure 4.11, at 2 hours, no activity occurred, and the methyl ester content started in initial 3 hours and slightly decreased until 7 hours. The decreased of methyl ester content at long reaction time due to the side reaction and reversible reaction occurred. However, further investigation would be needed to explore the mechanism in detail. On the other hand, at 3 hours the biodiesel yield remained nearly constant until 7 hours. The maximum methyl ester content and biodiesel yield obtained at 3 hours were 96.67 wt.% and 88.76 wt.%, respectively.

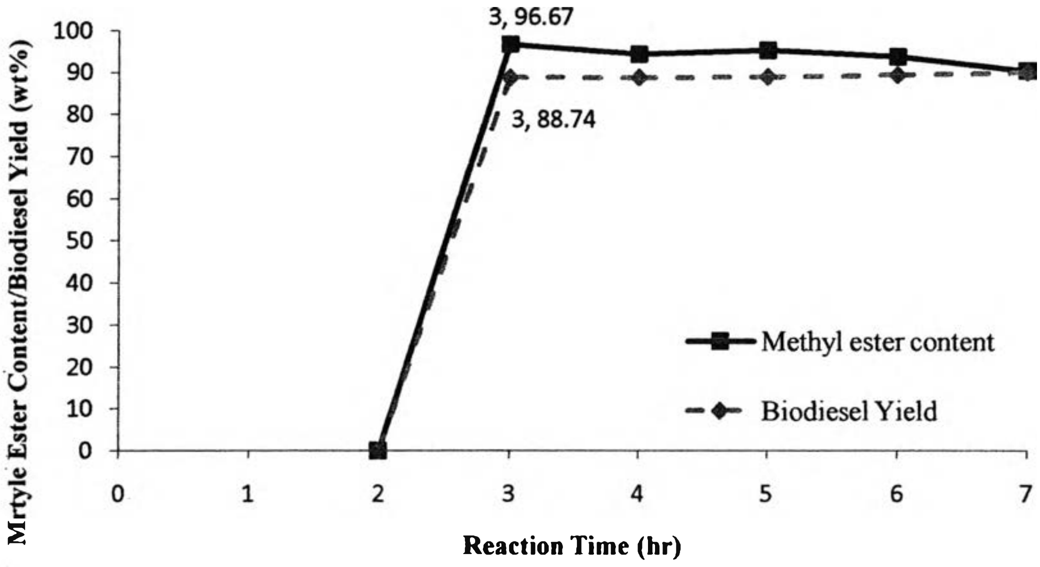

Figure 4.11 Influence of reaction time on the methyl ester content and biodiesel yield. Reaction condition: reaction temperature of 65°C, 20 wt.% loading amount of K with a molar ratio of methanol to oil of 15:1, 3 wt.% of the catalyst (base on weight of the vegetable oil), a stirrer speed of 300 rpm.

4.3.3 Influence of the Loading of K on the Methyl Ester Content and Biodiesel Yield

The effect of K loading on the biodiesel and methyl ester content was studied, as shown in Figure 4.12. The loading amount of K was varied in the range 5 to 40 wt.% at a reaction temperature of 65°C, 2 hours of reaction time at a molar ratio of methanol to oil of 15:1, 3 wt.% of the catalyst (base on weight of the vegetable oil), a stirrer speed of 300 rpm, and the size of KOH/ZrO_2 catalysts was 10-20 mesh. The results presented in Figure 4.10 showed that at low loading amount of K (5 wt.%), the KOH/ZrO_2 catalyst showed no activity and when increasing the K on ZrO_2 from 10 to 20 wt.%, the methyl ester content and biodiesel yield increased. When further increasing the amount of K loading on ZrO_2 from 25-40 wt.%, the methyl ester content and biodiesel yield were slightly decreased. The maximum methyl ester content was 94.74% for 20 wt.% loading of K on ZrO_2. From XRD result, it was found that at low loading amount of KOH, the basic sites were well dispersed on the surface. And when further increasing the K loading to 20 wt.%, a phase of K_2O was clearly observed. It can be explained that the presence of K_2O phase was cause of the high catalytic activity. However, when further increasing loading amount of K was over 25 wt.%, the methyl ester content decreased. It can be explained that which KOH loading was too high, the KOH could not be well dispersed and part of KOH could not be decomposed to K_2O. Moreover, the excess amount of KOH covered the active sites on the surface and hence the surface area decreased, therefore, the catalytic activity was decreased (Xie *et al.*, 2007). This result was supported by SEM-EDS result when increasing the K loading, the catalyst size was increased which lead to a decreased surface area.

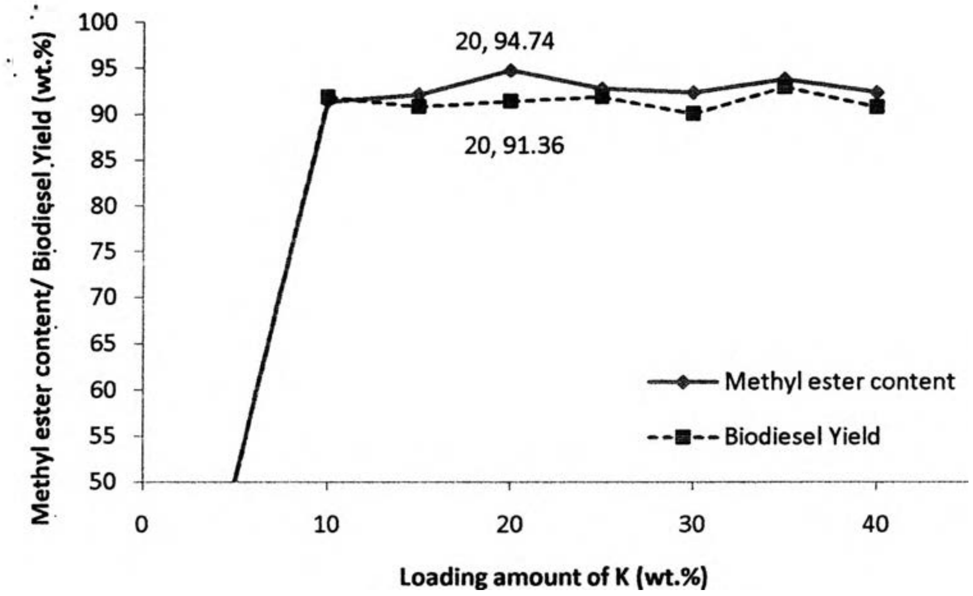

Figure 4.12 Influence of K loading on the methyl ester content and biodiesel yield. Reaction condition: reaction temperature of 65°C, 2 hours reaction time at a molar ratio of methanol to oil of 15:1, 3 wt.% of the catalyst (base on weight of the vegetable oil), a stirrer speed of 300 rpm, and the size of KOH/ZrO_2 catalysts was 10-20 mesh.

The dependence of activity of KOH/mordenite catalyst on the amount loading of KOH was investigated by varying the loading amount in the range 5 to 30 wt.% at a reaction temperature of 65°C, 3 hours reaction time at a molar ratio of methanol to oil of 15:1, 3 wt.% of the catalyst (base on weight of the vegetable oil), and a stirrer speed of 300 rpm. The results are illustrated in Figure 4.13. At 5 wt.% loading amount of K the KOH/mordenite catalyst showed no activity. The methyl ester content and biodiesel yield were increased when loading amount of K was increased from 10 wt.% to 20 wt.% afterward it remained constant until 25 wt.%. When the loading amount of K was increased to 30 wt.%, the methyl ester content rapidly decreased but the biodiesel yield remained constant. The highest methyl ester content of 96.81 wt.% was obtained from a loading of 25 wt.% K on mordenite. The suddenly reduction of methyl ester content at 30 wt.% because the high loading amount of KOH destroyed the structure of mordenite which can be observed from the physical characteristic. The catalysts had clear crystallite which differed from low loading amount of KOH. The XRD result confirmed this result, a small change of XRD pattern of 30 wt.% was noted.

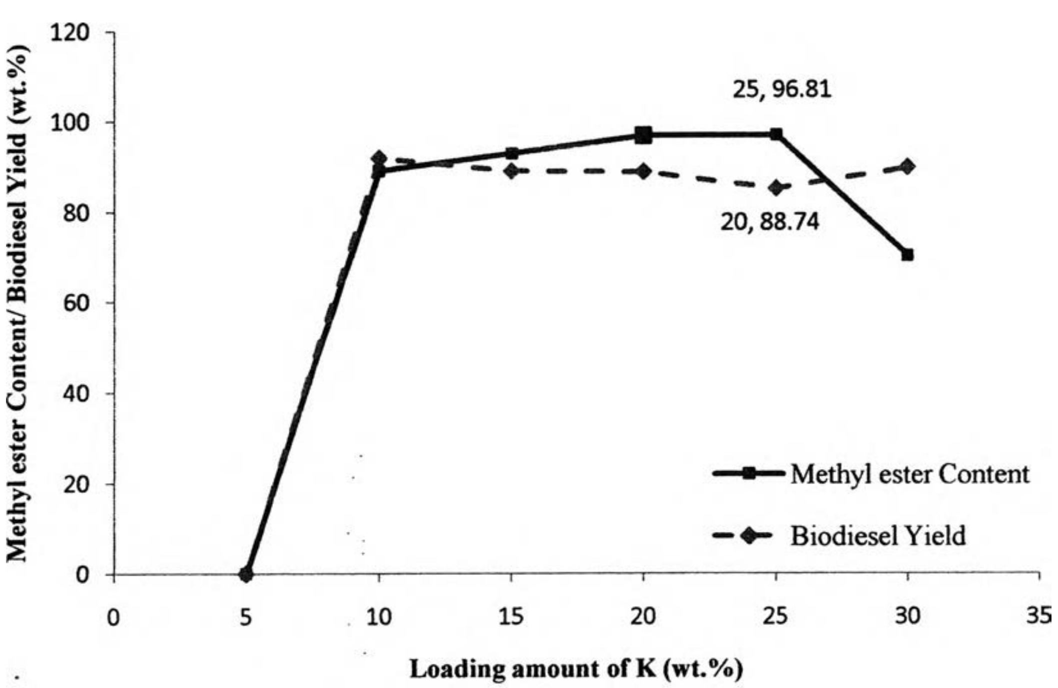

Figure 4.13 Influence of K loading on the methyl ester content and biodiesel yield. Reaction conditions: reaction temperature of 65°C, 3 hours reaction time at a molar ratio of methanol to oil of 15:1, 3 wt.% of the catalyst (base on weight of the vegetable oil), and a stirrer speed of 300 rpm.

4.3.4 Influence of Molar Ratio of Methanol/Oil on the Methyl Ester Content and Biodiesel Yield

Normally, transesterification reaction requires three moles of methanol for each triglyceride. Because transesterification is a reversible reaction, the excess methanol is needed to force the reaction shift to the right hand side. The effect of molar ratio of methanol/oil was studied by varying the molar ratio of methanol to oil from 6 to 21 at a reaction temperature of 65°C, 2 hours raction time, 20 % loading amount of K on ZrO_2 at a molar ratio of methanol to oil of 15:1, 3 wt.% of the catalyst (base on weight of the vegetable oil), a stirrer speed of 300 rpm, and the size of KOH/ZrO_2 catalysts was 10-20 mesh. As can be seen in Figure 4.14, the methyl ester content and biodiesel yield increased with increasing the molar ratio of methanol/oil from 6 to 15. The maximum methyl ester content of 94.74 wt.% was obtained at a methanol to oil molar ratio of 15:1. Beyond the molar ratio of 18:1, the methyl ester content decreased. At a high molar ratio of methanol/oil, glycerol phase occurred on the top phase resulting in difficulty to separate the products. These phenomena could be explained that the recombination of fatty acid methyl ester and glycerol occurred at the excess amount of methanol. The fatty acid methyl ester and glycerol are nearly immiscible solubility in fatty acid methyl ester, so the triglycerides conversion decreased (Shu *et al.*, 2007).

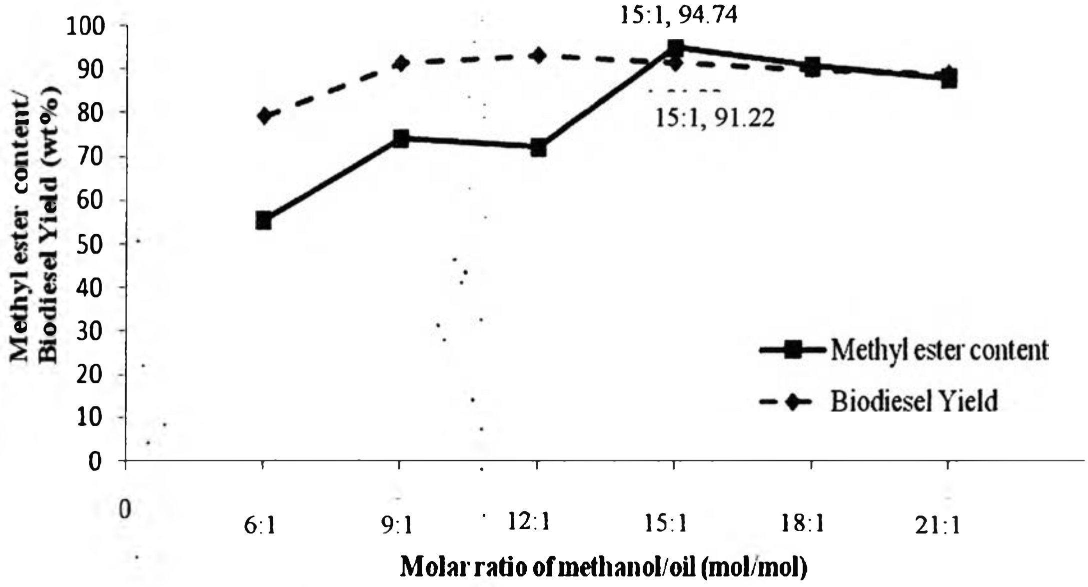

Figure 4.14 Influence of molar ratio of methanol to oil on the methyl ester content and biodiesel yield. Reaction conditions: reaction temperature of 65°C, 20 wt.% loading amount of K on ZrO_2, 2 hours reaction time, 3 wt.% of the catalyst (base on weight of the vegetable oil), a stirrer speed of 300 rpm, and the size of KOH/ZrO_2 catalysts was 10-20 mesh.

To investigate the effect of molar ratio of methanol/oil on KOH/mordenite catalyst, the experiment was carried out with various molar ratios of methanol/oil from 6 to 21. The reaction was carried out at a reaction temperature of 65°C, 20 % loading amount of K on mordenite support with 3 hours reaction time, 3 wt.% of the catalyst (base on weight of the vegetable oil), and stirrer speed of 300 rpm. As presented in Figure 4.15, when increasing the molar ratio of methanol/oil, the methyl ester content and biodiesel yield were increased considerably. At a 6:1 molar ratio, the methyl ester content and biodiesel yield were low due to interference of soap formation (Abigail *et al.*, 2003). Beyond the molar ratio of 12:1, the excessive amount of methanol had no significant effect on methyl ester content and biodiesel yield. The maximum methyl ester content of 96.67 wt.% obtained when molar ratio was very close to 15:1.

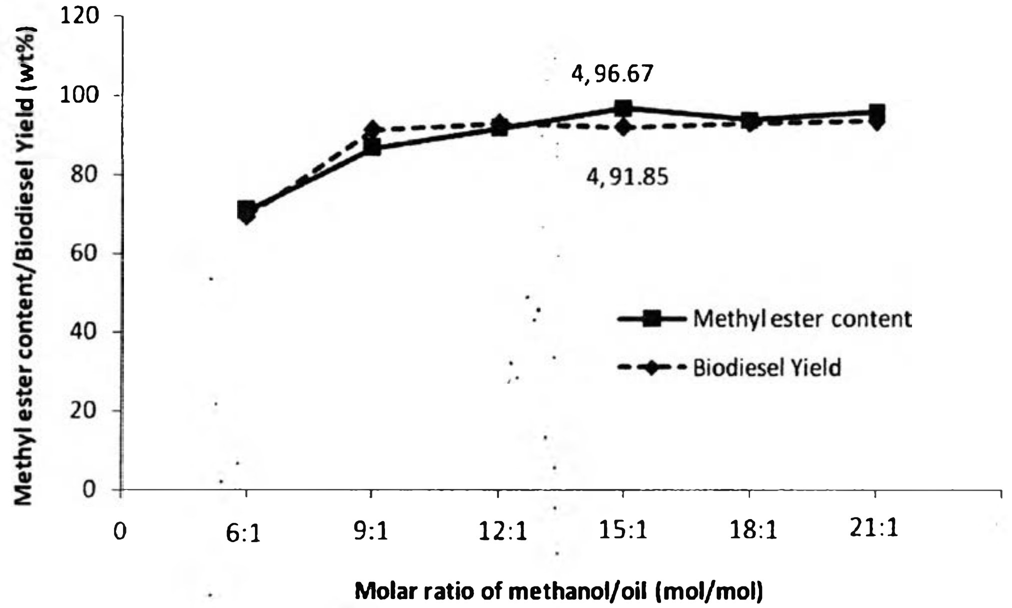

Figure 4.15 Influence of molar ratio of methanol to oil on the methyl ester content and biodiesel yield. Reaction conditions: 65 °C of reaction temperature, 3 hours reaction time, 20 wt.% loading K on mordenite, 3 wt.% of the catalyst (base on weight of the vegetable oil), and 300 rpm of stirrer speed.

4.3.5 Influence of Amount of Catalyst on Methyl Ester Content and Biodiesel Yield

The influence of catalyst amount on methyl ester content and biodiesel yield was investigated at the initial condition carried out at 65°C, 20 wt.% loading K on ZrO_2, 15:1 of molar ratio of methanol to oil, 300 rpm of stirrer speed, and the size of KOH/ZrO_2 catalysts was 10-20 mesh. The catalyst amount was varied in the range of 1-5 wt.% (base on vegetable oils). As shown in Figure 4.16, the methyl ester content of KOH/ZrO_2 catalyst was increased with increasing the amount of catalyst. The maximum methyl ester content of 99.69 wt.% was obtained at 5 wt.%. It can be suggested that at a high amount of catalyst, high amount of active sites are required to convert triglyceride to biodiesel.

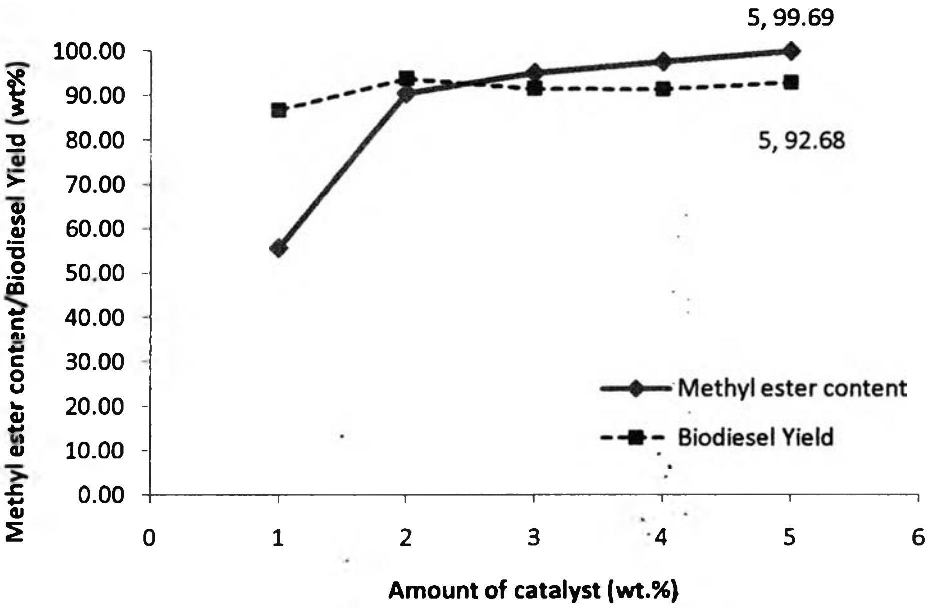

Figure 4.16 Influence of amount of catalyst on the methyl ester content and biodiesel yield. Reaction condition: 65 °C of reaction temperature, 2 hours reaction time, 20 wt.% loading K on ZrO_2 with a 15:1 molar ratio of methanol to oil, 300 rpm of stirrer speed, and the size of KOH/ZrO_2 catalysts was 10-20 mesh.

To study the effect of amount of KOH/mordenite catalyst, the catalyst was carried out at 65 °C of reaction temperature, 3 hours reaction time, 20 wt.% loading K on mordenite with a 15:1 molar ratio of methanol to oil and 300 rpm of stirrer speed by varying the amount of catalyst from 1 to 5 wt.%. The result shown in Figure 4.17 illustrated that the methyl ester content was increased firstly with increasing the catalyst amount from 1 to 4 wt.%. But further increasing the catalyst amount, the methyl ester content was decreased because a mixing problem of reactant, catalyst, and product. The products became too viscous and required demand of high power consumption for adequate stirring (Kim *et al.*, 2004). The maximum methyl ester content of 98.40 wt.% was obtained at 4 wt.% of catalyst.

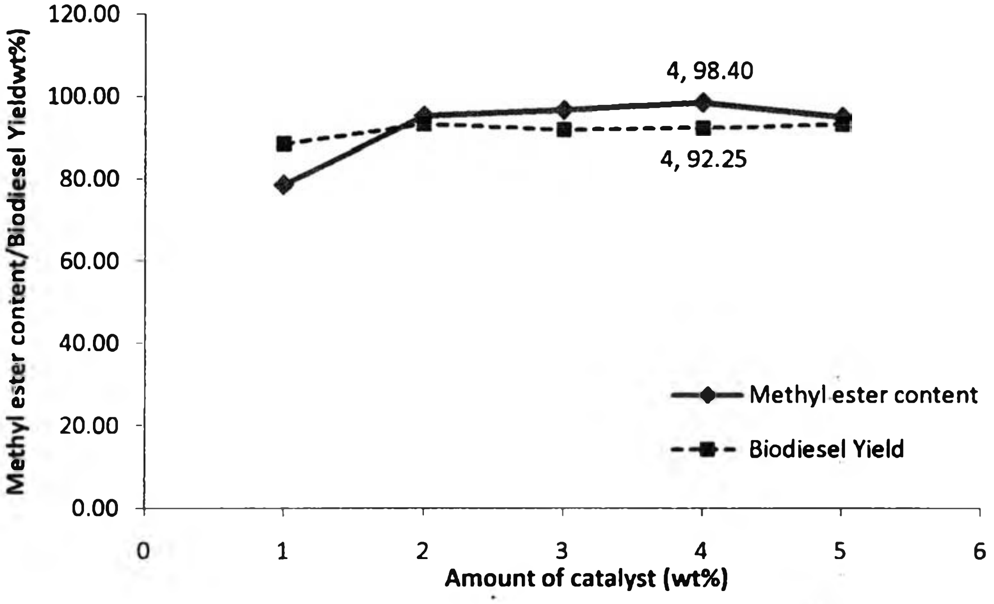

Figure 4.17 Influence of amount of catalyst on the methyl ester content and biodiesel yield. Reaction condition: 65 °C of reaction temperature, 3 hours reaction time, 20 wt.% loading K on mordenite with a 15:1 molar ratio of methanol to oil and 300 rpm of stirrer speed.

4.3.6 Influence of Calcination Temperature on Methyl Ester Content

The influence of calcination temperature after impregnation on the methyl ester content and biodiesel yield had been investigated within the range of 400 to 600°C. The reaction condition was 65 °C of reaction temperature, 3 hours of reaction time, 20 wt.% loading K on mordenite with a 15:1 molar ratio of methanol to oil and 300 rpm of stirrer speed. Figure 4.18 illustrates that when increasing calcination temperature, the methyl ester content decreased because at high calcined temperature, the catalyst loss the catalytic activity. Xie and coworkers explained that the decreased catalytic activity at high temperatures because of the loss potassium species by evaporation or sublimation into the surface. From the XRD and SEM results showed that the structure of mordenite was collapsed which lead to the decreased catalytic activity. Uncalcined catalyst gave the highest methyl ester content of 96.67 wt.%.

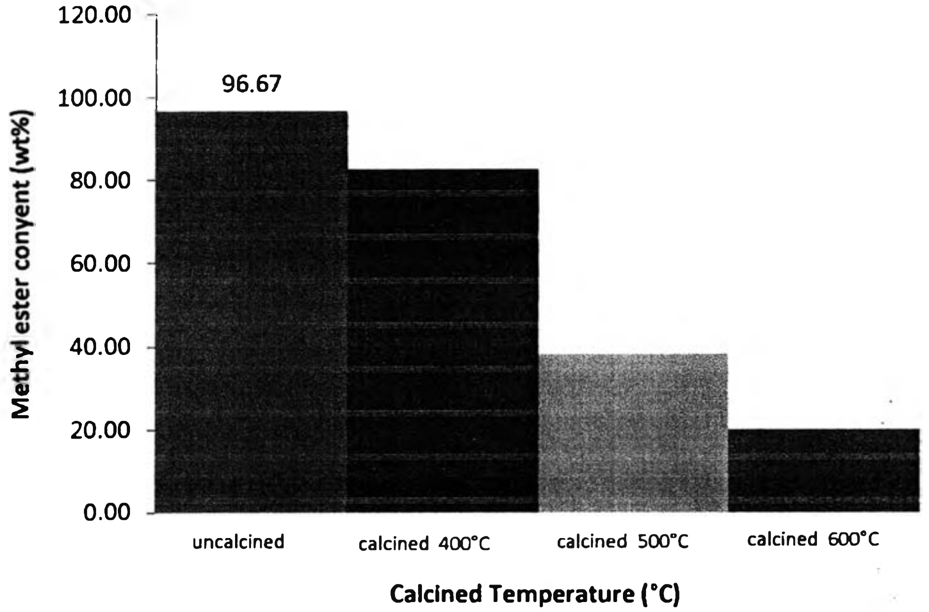

Figure 4.18 Influence of calcination temperature on the methyl ester content. Reaction condition: 65 °C of reaction temperature, 3 hours of reaction time, 20 wt.% loading K on Mordenite with a 15:1 molar ratio of methanol to oil, 3 wt.% of the catalyst (base on weight of the vegetable oil), and 300 rpm of stirrer speed.

4.4 Recycle Catalyst

4.4.1 Spent KOH/ZrO_2 Catalyst

4.4.1.1 XRD Patterns of Spent KOH/ZrO_2 Catalysts

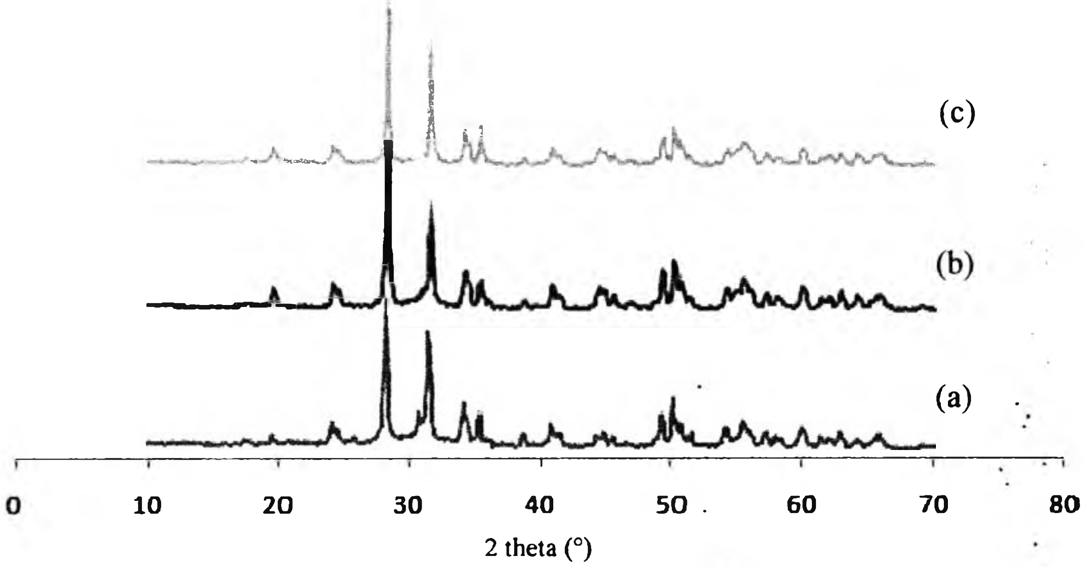

Figure 4.19 XRD patterns of the fresh KOH/ZrO_2 catalysts and spent KOH/ZrO_2 catalysts: (a) Fresh 20 wt.% K/ZrO_2, (b)Spent 1st 20 wt.% K/ZrO_2, (c) Spent 2nd 20 wt.% K/ZrO_2.

The XRD pattern of fresh and spent catalysts are compared in Figure 4.19. The XRD diffraction of spent catalyst showed no significant difference when compared to the fresh catalyst. But the diffraction of spent catalyst at 2θ= 31°, the peak of K_2O disappreared. The disappeared peak can be suggested that the KOH which active site might leach from the surface. Morover, the intensity of ziconia peak increased with increasing the number of run.

4.4.1.2 SEM Results of Spent KOH/ZrO$_2$ Catalysts

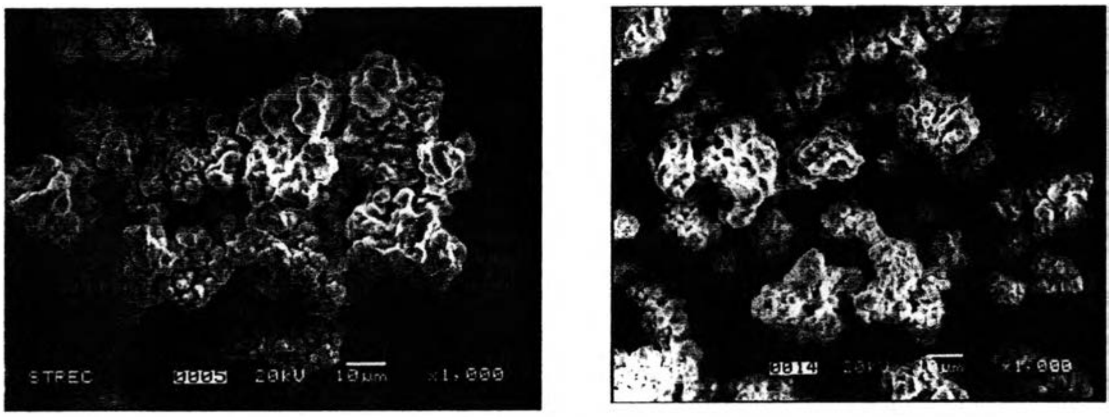

(a) Fresh 20 wt.% K/ZrO$_2$ (b) Spent 1st 20 wt.% K/ZrO$_2$

(c) Spent 2nd 20 wt.% K/ZrO$_2$

Figure 4.20 SEM images of fresh KOH/ZrO$_2$ and spent KOH/ZrO$_2$ catalyst.

The SEM image of the fresh 20 wt.% K on ZrO$_2$ was compared to that the spent catalysts, as shown in Figure 4.20. The SEM pictures illustrate that the particles sizes of the spent catalyst were smaller than the fresh catalyst. As a result, the size of fresh KOH/ZrO$_2$ catalyst was 10-50 µm, in the first run the particle size of the catalyst was decreased to 5-15 µm, and by 1-5 µm in the second run. And the surface area of spent catalyst was higher than that of fresh catalyst because the catalyst was destroyed by stirring.

Table 4.3 The leaching and methyl ester content of spent KOH/ZrO_2 catalyst

Type of Catalyst	**Percent K element (EDS)**	**Percent K element (XRF)**	**% Leaching**	**Methyl ester content (wt.%)**
20% K/ZrO_2	14.42	25.27	-	94.74
Spent1st 20% K/ZrO_2	8.61	14.02	44.52	1.19
Spent2nd 20% K/ZrO_2	1.61	10.84	81.26	-

After the reaction was completed, the catalyst was separated and used to study the catalyst lifetime without pretreatment or activation. The fresh palm oil and methanol were used in the same amounts as the initial condition. Table 4.3 displays the methyl ester content and the run number of the 20 wt.% K on ZrO_2. A remarkable reduction in catalytic performance was observed, yielding 1.19 wt.% of methyl ester contents in the second run for KOH/ZrO_2 catalyst. The rapidly decreased of methyl ester content on KOH/ZrO_2 catalyst implies that part of the potassium initially deposited onto the catalyst is leached from the solid (44.52% and 81.26%) which was subsequently confirmed by the results of XRF and EDS of the spent catalysts, as shown in Table 4.1. The percentage of potassium for first and second run was much lower than fresh catalyst due to the large absorbed liquid phase (oil, methanol, methyl ester, and glycerin) (Alonso *et al.*, 2007).

4.4.2 Spent KOH/mordenite Catalyst

4.4.2.1 XRD Patterns of Spent KOH/mordenite Catalysts

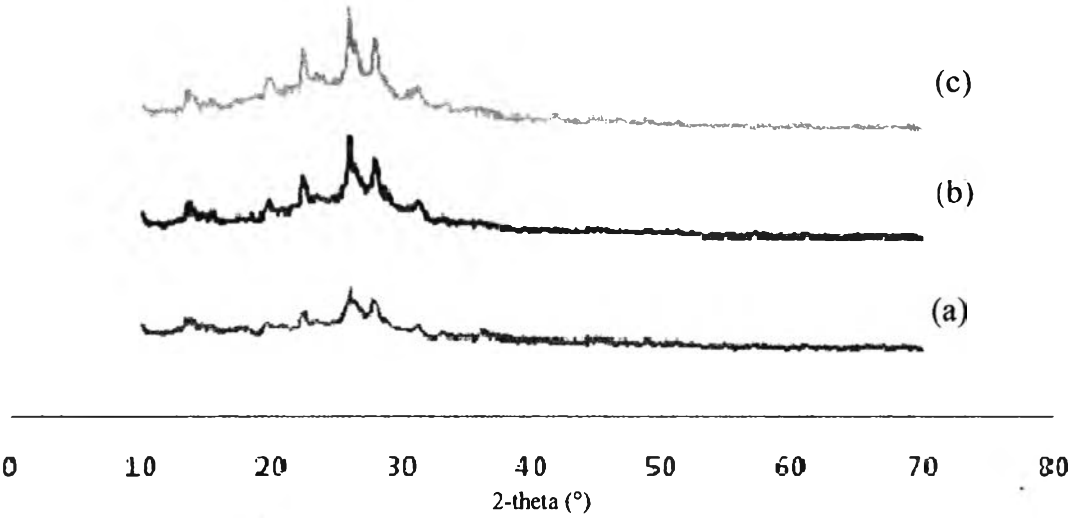

Figure 4.21 XRD patterns of the fresh KOH/mordenite catalysts and spent KOH/mordenite catalysts: (a) mordenite, (b) Fresh 20 wt.% K on mordenite, (c) Spent 20 wt.% K/ on mordenite.

Figure 4.21 illustrates the comparison of XRD pattern of fresh KOH/mordenite and spent KOH/mordenite catalysts. The XRD pattern of spent catalyst was almost the same as the XRD pattern of fresh catalyst; however, a higher intensity of XRD pattern of spent catalyst was observed, most probably due to the particles shape. It is attributed to the losses of active site and surface area.

4.4.2.2 SEM Result of Spent KOH/mordenite Catalysts

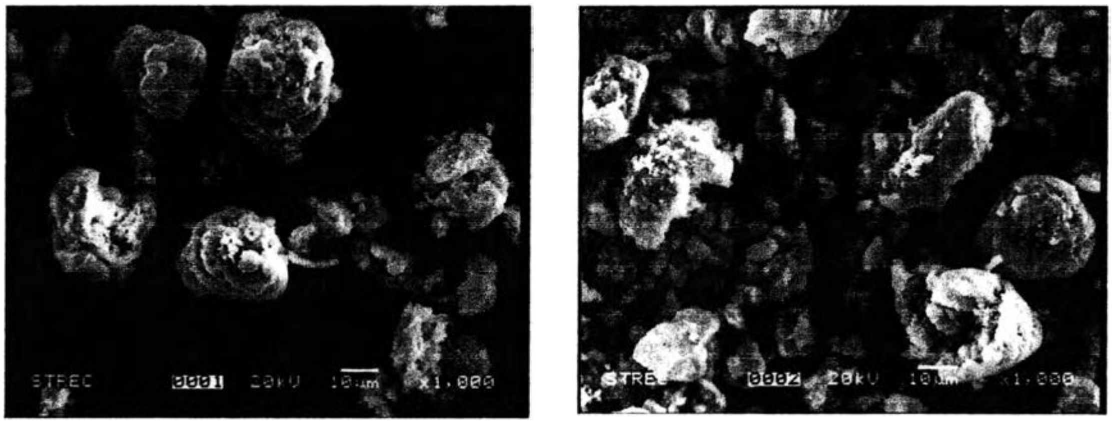

(a) Fresh 20 wt.% K/mordenite (b) Spent 1st 20 wt.% K/mordenite

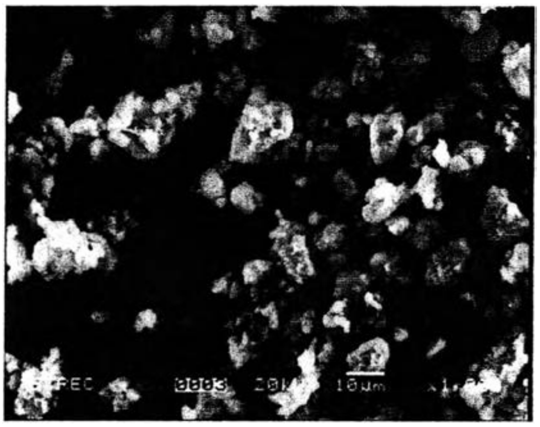

(c) Spent 2nd 20 wt.% K/mordenite

Figure 4.22 SEM images of fresh KOH/mordenite and spent KOH/mordenite catalysts.

The morphologies of fresh KOH/mordenite and spent KOH/mordenite catalysts are shown in Figure 4.22, The size of fresh KOH/mordenite was 20-30 µm. In the first run the size of catalyst decreased in size by 10-20 µm, and decreased in size by 7-10 µm in the second run. The result showed that the size slightly decreased, it can be suggested that KOH on the catalyst might be leached out from the catalyst or the catalyst might be destroyed by stirring.

Table 4.4 The leaching and methyl ester content of spent KOH/mordenite catalyst.

Type of Catalyst	**Percent K element (EDS)**	**Percent K element (XRF)**	**% Leaching**	**Methyl ester content (wt%)**
20%KOH/Mordenite	13.49	26.44	-	96.67
Spent1st 20%KOH/Mordenite	11.21	23.63	10.63	72.33
Spent2nd 20%KOH/Mordenite	8.76	21.77	7.87	-

Table 4.4 displays the methyl ester content and the run number of the 20 wt.% K/mordenite. A remarkable reduction in catalytic performance was observed, yielding 72.33 wt.% of methyl ester contents in the second run for KOH/mordenite catalyst. The decrease of the methyl ester content can be suggested that methanol or methyl ester covered the basic site which decreased the catalytic activity of the catalyst. The XRF and EDS results showed that the percentage of potassium decreased with increasing the number of runs. The potassium leaching on KOH/mordenite were 10.63% and 7.87% in the first and second run, respectively. It can be suggested that the active species were slightly leached from the solid support which reveals a lack of chemical stability of the catalysts (Arzamendi *et al.*, 2007). Howev er, the EDS instrument might be not reliable because it could not present the bulk composition.